Observational Study

Medicine®

OPEN

Quantitative analysis of vascularity for thyroid nodules on ultrasound using superb microvascular imaging

Can nodular vascularity differentiate between malignant and benign thyroid nodules?

Min Ji Hong, MD[a], Hye Shin Ahn, MD[a,*], Su Min Ha, MD[b], Hyun Jeong Park, MD[a], Jiyun Oh, MD[a]

Abstract

This study aimed to investigate the utility of adding superb microvascular imaging (SMI) to B-mode ultrasound (US) for distinguishing between benign and malignant thyroid nodules and evaluate the usefulness of SMI quantification of nodular vascularity for diagnosing thyroid cancer.

The malignancy likelihood was scored for 3 datasets before versus after additional color Doppler imaging or SMI using 4-scale visual analysis (i.e., B-mode US alone, B-mode US + color Doppler image, and B-mode US + SMI). Further, the SMI pixel count was measured in the region of interest, including the whole nodule, on the longitudinal view. It was compared between benign and malignant nodules and analyzed according to the US patterns of thyroid nodules based on the Korean thyroid imaging reporting and data system. We calculated the area under the receiver operating characteristic curve values, sensitivities, and specificities.

There was no significant difference in the area under the receiver operating characteristic curve values among B-mode, B-mode + color Doppler, and B-mode + SMI. However, the SMI pixel count was significantly higher in malignant thyroid nodules than in benign ones. The optimal cut-off value for the SMI pixel count for predicting malignant thyroid nodules obtained using a receiver operating characteristic curve was 17 (40.54% in sensitivity, 91.3% in specificity). Analysis based on the US pattern of thyroid nodules revealed significant differences in the nodules with low-to-intermediate suspicious US features between malignant and benign nodules.

Quantification analysis of vascularity using SMI can differentiate malignant thyroid nodules from benign ones.

Abbreviations: AUC = area under the receiver operating characteristic curve, CNB = core needle biopsy, FNA = fine-needle aspiration, SMI = superb microvascular imaging, TI-RADS = thyroid imaging reporting and data system.

Keywords: superb microvascular imaging, thyroid nodule, ultrasonography

1. Introduction

In recent times, the introduction of high resolution US as diagnostic and therapeutic tool for various medical field has made it possible to manage advanced local disease.[1,2] Especially, thyroid ultrasonography (US) is the standard imaging modality for sensitive and low-cost evaluation of thyroid nodules. It can differentiate between malignant and benign thyroid nodules, as well as guide fine-needle aspiration (FNA) for nodules suspected to be malignant.[3,4] Numerous guidelines have suggested highly suspicious US features for predicting thyroid cancer, including marked hypoechogenicity, spiculated or microlobulated margin, microcalcifications, and a taller-than-wider shape.[5–9] Although

Editor: Neeraj Lalwani.

This research was supported by the Chung-Ang University Research Grants in 2019.

All procedures performed in studies involving human participants were in accordance with the ethical standards of the institutional and/or national research committee and with the 1964 Helsinki declaration and its later amendments or comparable ethical standards.

Informed consent was waived due to retrospective study design.

The authors have no conflicts of interests to disclose.

All data generated or analyzed during this study are included in this published article [and its supplementary information files].

[a] *Department of Radiology, Chung-Ang University Hospital, Chung-Ang University College of Medicine, Seoul, Republic of Korea,* [b] *Department of Radiology, Seoul National University Hospital, Seoul University College of Medicine, Seoul, Republic of Korea.*

[*] *Correspondence: Hye Shin Ahn, Department of Radiology, Chung-Ang University Hospital, Chung-Ang University College of Medicine, 84 Heukseok-Ro, Dongjak-Gu, Seoul 06973, Republic of Korea (e-mail: ach0224@gmail.com).*

How to cite this article: Hong MJ, Ahn HS, Ha SM, Park HJ, Oh J. Quantitative analysis of vascularity for thyroid nodules on ultrasound using superb microvascular imaging: can nodular vascularity differentiate between malignant and benign thyroid nodules?. Medicine 2022;101:5(e28725).

Received: 26 November 2020 / Received in final form: 23 December 2021 / Accepted: 11 January 2022

http://dx.doi.org/10.1097/MD.0000000000028725

representative US features for malignant thyroid nodules have been suggested, there are considerable variations in the reported diagnostic performance of ultrasonography. Moreover, none of these US features have sufficient specificity for classifying thyroid cancer.

Doppler US is widely used for differential diagnosis of benign and malignant thyroid nodules to evaluate the thyroid nodule vascularity. The rationale for studying thyroid nodule vascularity involves the correlation of cellular proliferation with increased vascularization, which may contribute to the anarchical angiogenesis observed in malignancy.[10,11] A recent review article indicated that color Doppler US has acceptable diagnostic performance and may be useful for predicting malignant thyroid nodules.[12] Specifically, it indicated that marked intranodular vascularity on color Doppler US is a significant predictor of thyroid nodule malignancy. Superb microvascular imaging (SMI) is a recently developed technique for microvascular flow imaging.[13–16] SMI analyzes clutter motion and employs advanced clutter suppression to extract flow signals from large-to-small vessels, which allows superior visualization of low-velocity flow.[13] Recent articles have indicated that SMI is more accurate than Doppler US for assessing malignant thyroid nodules; moreover, SMI findings of a large vessel number or intranodular flow are associated with thyroid nodule malignancy.[14–16] Qualitative comparison by these studies has demonstrated SMI as an emerging additional modality to conventional US. However, quantification vascularity analysis of thyroid nodules using the SMI technique has not been performed. Therefore, this study aimed to investigate the utility of additional SMI to B-mode US for distinguishing between benign and malignant thyroid nodules and to evaluate the usefulness of SMI quantification for nodular vascularity to diagnose thyroid cancer.

2. Materials and methods

2.1. Patients and lesions

This study was approved by the institutional review board (H-2010-007-19335). The requirement for informed consent was waived because of the retrospective study design. Between April 2018 and July 2018, we selected 180 initially detected thyroid nodules from 136 patients who underwent initial FNA or core needle biopsy (CNB) at our institution. Among them, 120 nodules from 134 patients were excluded for lacking final diagnoses. Finally, we included 60 consecutive nodules (≥0.5 cm) from 52 patients with final diagnoses (42 women, 10 men; mean age = 51.2 ± 11.9 years). Final malignancy diagnoses were determined through (i) histopathological diagnosis using surgical resections and (ii) malignancy findings on FNA or CNB. Final benign diagnoses were determined through (i) histopathological diagnosis using surgical resections, (ii) at least two benign diagnoses on FNA or CNB, and (iii) an initial benign result on FNA or CNB with a stable or decreased nodule size on US after ≥12 follow-up months.

2.2. Ultrasonographic examinations and US-guided procedures

One of 2 radiologists with 6 and 4 years of experience in thyroid US, respectively, performed conventional US examinations. After B-mode US, patients scheduled to undergo US-guided FNA underwent color Doppler and SMI conducted by a radiologist with 6 years of experience in thyroid US using a high-resolution equipment with a 14-MHz probe (Aplio 500, Canon Medical Systems Corporation).

B-mode US images were initially acquired followed by color Doppler and SMI images in the same plane without altering the patient's position. Color and monochrome SMI were performed for nodules and the focal zone by maintaining a constant scanning depth and time-gain compensation to optimize target region visualization. Transverse and sagittal still images and approximately 10-s cine images were acquired for all nodules. A rectangular region of interest (ROI) was focused on the target lesion and adjusted to include surrounding normal thyroid and adjacent muscles. The US parameters for SMI were as follows: color velocity scale: 1.0 to 2.0 cm/s, color frequency: 14 MHz, SMI gain: 32, enhanced vascular information by time smoothing adjustment.

US-guided FNA was conducted using a 23-gauge needle attached to a 5-mL syringe. Successful sampling was allowed by numerous multidirectional passes through the nodule. Specimens were preserved in bottles with 95% ethanol for liquid-based cytological examination. Repeat biopsy was prompted by nondiagnostic cytological findings of nodules or atypia/follicular lesions of undetermined significance. US-guided CNB was conducted using a free-hand technique with an 18-gauge dual-action semiautomatic core biopsy needle with a 22-mm throw. Specimens obtained through FNA and CNB were examined by a thyroid pathologist with 17 years of experience. FNA interpretation was based on the Bethesda System for Reporting Thyroid Cytopathology[17] while CNB results were diagnosed using a six-tier pathology reporting system.[18]

2.3. Data and statistical analysis

Two experienced radiologists blinded to the cytology results analyzed still images and cine loops of thyroid nodules from the US examinations, including the Color Doppler and SMI images. Two reviewers with 8 and 9 years of thyroid imaging experience, respectively, performed image analyses in consensus. Nodules on B-mode US were categorized based on the Korean thyroid imaging reporting and data system (K-TIRADS).[5] Color Doppler and SMI images were visually assessed using a 4-point scale. Nodular vascularity on color Doppler and SMI was classified according to the scoring system recommended by Chung et al[12] (Fig. 1). A score of 1 indicated absent nodule vascularity (no vascularity); a score of 2 indicated the presence of circumferential vascularity at the nodular margin (perinodular vascularity only); a score of 3 indicated mild intranodular vascularity with or without perinodular vascularity (vascularity <50%); and a score of 4 indicated marked intranodular vascularity with or without perinodular vascularity (vascularity >50%). Nodular vascularity quantification was performed using in-house software for SMI images (an in-house program for Pixel count [VITestApp] by Canon Medical Systems). We chose color-coded SMI over monochromatic SMI since automatic quantification was feasible only in the color-coded SMI images. For quantitative measurement, the ROI was carefully set at the nodular periphery to include the whole nodule using the manual drawing method. For cases with predominantly cystic nodules, only the solid component was measured for quantification. Upon setting of the ROI, the pixels showing the flow signal were automatically counted (Fig. 2). The ROI was drawn thrice for each patient on the longitudinal scan and the average pixel count was recorded.

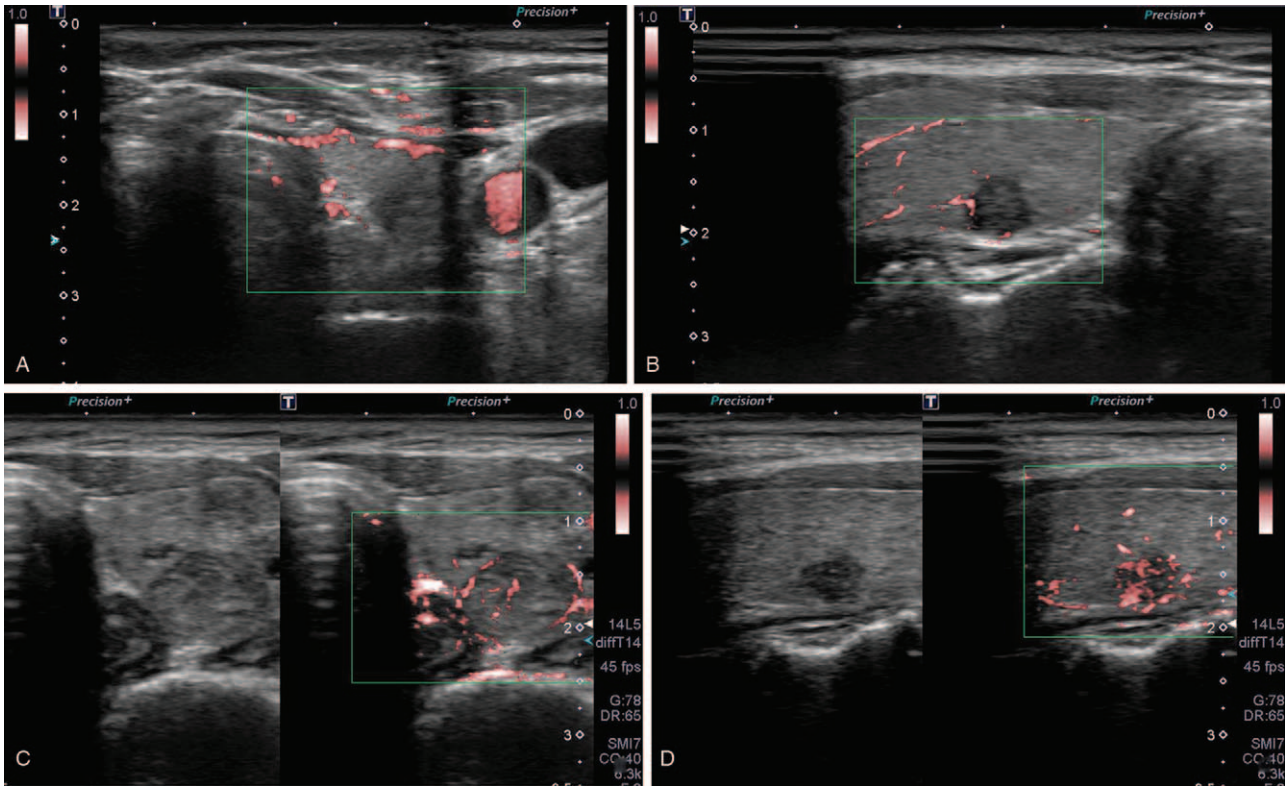

Figure 1. Ultrasonographic images of the general appearance of thyroid nodules for superb microvascular imaging scores 1, 2, 3, and 4. (A) The nodular interior reveals the absence of nodule vascularity (score 1). (B) The nodule reveals perinodular vascularity only (score 2). (C) The nodule reveals mild intranodular vascularity with or without perinodular vascularity (score 3). (D) The nodule reveals marked intranodular vascularity with or without perinodular vascularity (score 4).

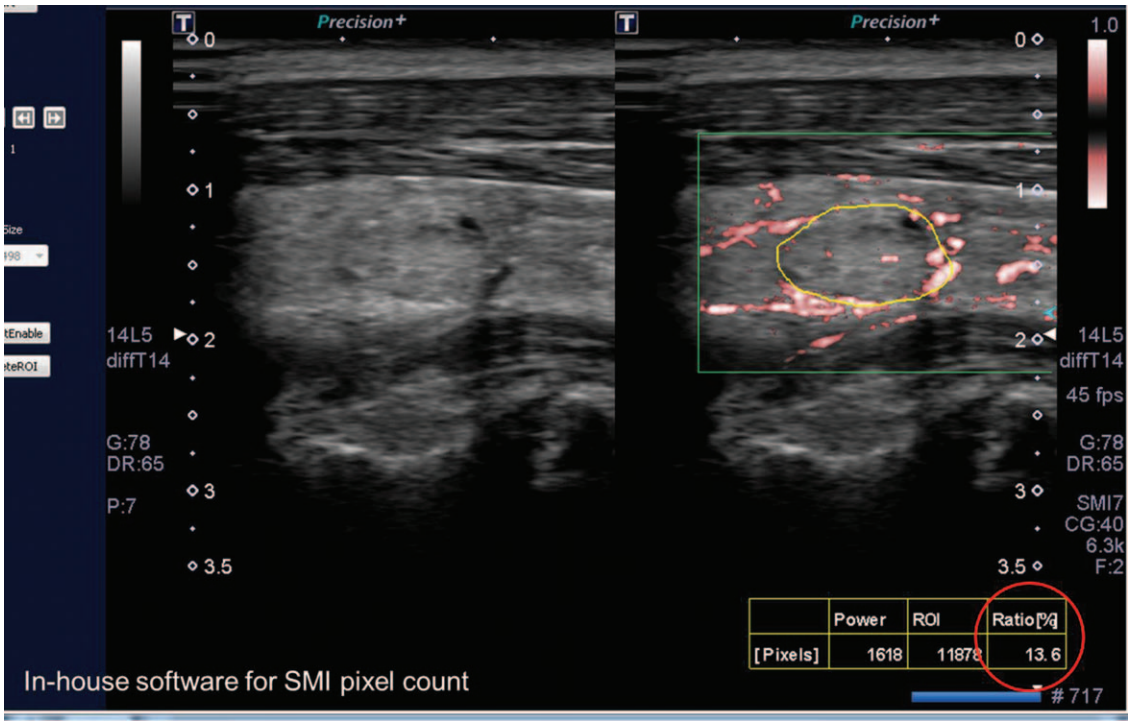

Figure 2. An example of the SMI pixel count and its quantification for thyroid nodule microvascularity. The reviewer manually drew the region of interest to include the whole nodule on the longitudinal view. The in-house software automatically measured the flow signal within the nodule.

To evaluate the diagnostic performance of the 3 data sets (i.e., B-mode US alone, B-mode US + color Doppler, and B-mode ultrasonography + SMI) for distinguishing between benign and malignant thyroid nodules, the malignancy likelihood (0-100) for each data set was scored. First, based on the K-TIRADS guideline,[5] the nodules were categorized into 3 groups (low [KT3], intermediate [KT4], high suspicious [KT5]). Subsequently, the malignancy likelihood for thyroid nodule was assessed on B-mode US. The range of malignancy risk was based on the K-TIRADS, where the scores for KT3, KT4, and KT5 were 3–15, 15–50, >60, respectively. The malignancy scores for each nodule was determined after the color Doppler or SMI addition to B-mode US through 4-scale visual assessment, within the ranges of malignancy risk for each thyroid nodule category. The mean values obtained from 2 reviewers were used for analyses given the previously reported excellent between-reviewer agreement.[19] The receiver operating characteristic (ROC) curve, area under the ROC curve (AUC) values, sensitivities, and specificities for malignancy in each data set were compared. Regarding vascularity quantification, we calculated the ROC curve and AUC values for the SMI pixel count and compared them between benign and malignant nodules. Moreover, the optimal cut-off points yielding the maximal sum of sensitivity and specificity were calculated. Further, the SMI pixel count was analyzed according to the US patterns of thyroid nodules (KT3/4 vs KT5). All statistical analyses were performed using commercially available software (IBM SPSS Statistics for Windows, Version 22.0; IBM Corp., Armonk, NY and MedCalc software, Version 16.4.1; MedCalc Software bvba, Ostend, Belgium). Statistical significance was set at $P < .05$.

3. Results

Among 60 thyroid nodules, 23 and 37 were benign and malignant, respectively. The lesion diameter on B-mode US ranged from 0.5 cm to 5.4 cm (mean: 1.9 cm). Surgical confirmation was conducted for 42 nodules; among them, the malignant lesions comprised 28 papillary carcinomas and 2 follicular carcinomas while the benign lesions comprised 5 nodular hyperplasias, 6 follicular adenomas, and 1 thyroiditis (Table 1). The lesions were assigned according to the K-TIRADS as follows: low (n = 26, 43.3%), intermediate (n = 19, 31.6%), high suspicion nodules (n = 15, 25%).

Table 2 summarizes the reviewers' ratings regarding the malignancy likelihood of nodules that underwent B-mode US only, B-mode US + color Doppler, and B-mode US + SMI. The final diagnosis showed that benign and malignant nodules had significant differences in the malignancy likelihood of all 3 data sets. Regarding AUC values, compared with B-mode US alone, the combined use of US with color Doppler or SMI improved the diagnostic performance for distinguishing between benign and malignant nodules. Among the 3 data sets, B-mode US + SMI had the highest AUC value (0.825; range: 0.705–0.911). However, it was not significantly higher than those of B-mode US alone (0.817; range: 0.696–0.905) and B-mode US + color Doppler (0.800; range: 0.676–0.892) (Fig. 3, ROC curve). There were no significant differences between B-mode US alone and B-mode US + color Doppler ($P = .665$), as well as between B-mode US alone and B-mode US + SMI ($P = .834$) (Figs. 4 and 5, PPT benign and malignant case).

Vascular quantification using in-house pixel count software revealed that malignant thyroid nodules had significantly higher vascularity (Table 3). The mean values of benign and malignant nodules were 10.84 ± 9.47 and 17.94 ± 12.53, respectively ($P = .038$). When using the optimal cut-off values that yield the maximal sum of sensitivity and specificity (cut-off value of 17), the sensitivity and specificity for malignancy were 40.54% and 91.3%, respectively (Fig. 6, ROC curve). In the analysis according to the US pattern of thyroid nodules, malignant nodules with KT3/4 US features had significantly higher SMI pixel counts compared with benign nodules with KT3/4 US features (benign: 10.84 ± 9.47, malignant: 17.94 ± 12.53, $P = .038$). However, in the nodules with KT5 US features, there was no significant difference in the SMI pixel count between benign and malignant nodules (benign: 9.2, malignant: 14.3 ± 13.58; $P = .723$) (Table 4).

Table 1

Demographic Data of 60 Nodules with final diagnoses.

Characteristic	Data
Age (mean ± SD, yrs)	51.2 ± 11.9
Sex (F:M)	42:10
Nodule size (mean ± SD, mm)	19.2 ± 8.9
Final diagnosis	
Benign	23 (38.3)
Surgery	12 (52.2)
Nodular hyperplasia	5 (21.7)
Follicular adenoma	6 (26.1)
Thyroiditis	1 (4.3)
At least two benign diagnoses on FNA or CNB	10 (43.5)
A benign result on FNA or CNB with follow-up US	1 (4.3)
Malignancy	37 (61.7)
Surgery	30 (81.1)
Papillary thyroid carcinoma	28 (75.7)
Classic	18 (64.3)
Follicular variant	9 (32.1)
Columnar cell variant	1 (3.6)
Follicular carcinoma	2 (5.4)
Malignant result on FNA or CNB	7 (18.9)

Numbers in parentheses are percentages.
CNB = core needle biopsy, FNA = fine-needle aspiration, SD = standard deviation, US = ultrasonography.

4. Discussion

In our study, all data sets (B-mode US, B-mode US + color Doppler, and B-mode US + SMI) revealed significant differences

Table 2

Comparison of the malignancy likelihood of thyroid nodules.

Variable	B-mode US	B-mode US + color doppler	B-mode US + SMI
Benign (mean ± SD)	19.87 ± 14.70	23.91 ± 19.17	24.87 ± 19.70
Malignant (mean ± SD)	53.46 ± 28.29	52.24 ± 25.04	57.54 ± 26.16
P value	<.001	<.001	<.001
Sensitivity (%)	73.0†	78.4†	62.2‡
Specificity (%)	87.0†	82.6†	91.3‡
AUC	0.817	0.800	0.825
	(0.696–0.905)	(0.676–0.892)	(0.705–0.911)
P value*		.665	.834

AUC = area under the receiver operating characteristic curve, SD = standard deviation, SMI = superb microvascular imaging, US = ultrasonography.
* Comparison of AUC with B-mode US value.
† Cut-off value (maximal value by Youden index) = 30.
‡ Cut-off value (maximal value by Youden index) = 50.

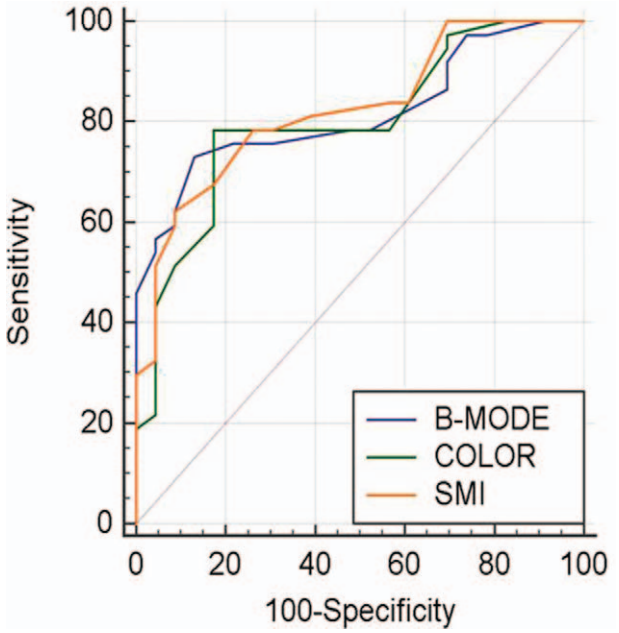

Figure 3. Results of the area under the receiver operating characteristic curve of the malignancy likelihood of thyroid nodules for differentiating between benign and malignant nodules.

between benign and malignant nodules. Although B-mode US + SMI had the highest AUC value, there were no significant differences among the data sets. Numerous studies have demonstrated good performance of color Doppler[20–22] and SMI[14–16] in diagnosing thyroid nodule malignancy. In clinical practice, the Doppler technique is an additional technique for improving specificity to differentiate benign from malignant nodules. Therefore, the present study design is consistent with clinical actualities. However, we did not observe significant differences among the data sets. The reason for this result is unclear; however, we used a malignancy likelihood ranging from 0 to 100 to compare data sets using the range of malignancy risk within the K-TIRADS category (low suspicion nodule [KT3]: 3–15, intermediate suspicion nodule [KT4]: 15–50, high suspicion nodule [KT5] >60). Moreover, visual assessment of color Doppler and SMI was performed using a 4-point scale. Therefore, the ROC curve and AUC values might not reflect the detailed differences between color Doppler and SMI. Nevertheless, there were significant differences in the SMI pixel count between benign and malignant thyroid nodules. The mean pixel count of malignant nodules was higher than that of benign ones. Furthermore, a pixel count of 17 was the optimal cut-off value for points yielding the maximal sum of sensitivity and specificity. For analysis according to the US pattern of thyroid nodules, SMI quantification could contribute toward predicting malignancy in low-to-intermediate suspicious nodules (KT3/4).

Conventional color Doppler US has disadvantages with respect to detailed descriptions of slow and microvascular flow. However, the recently developed SMI technique is a type of

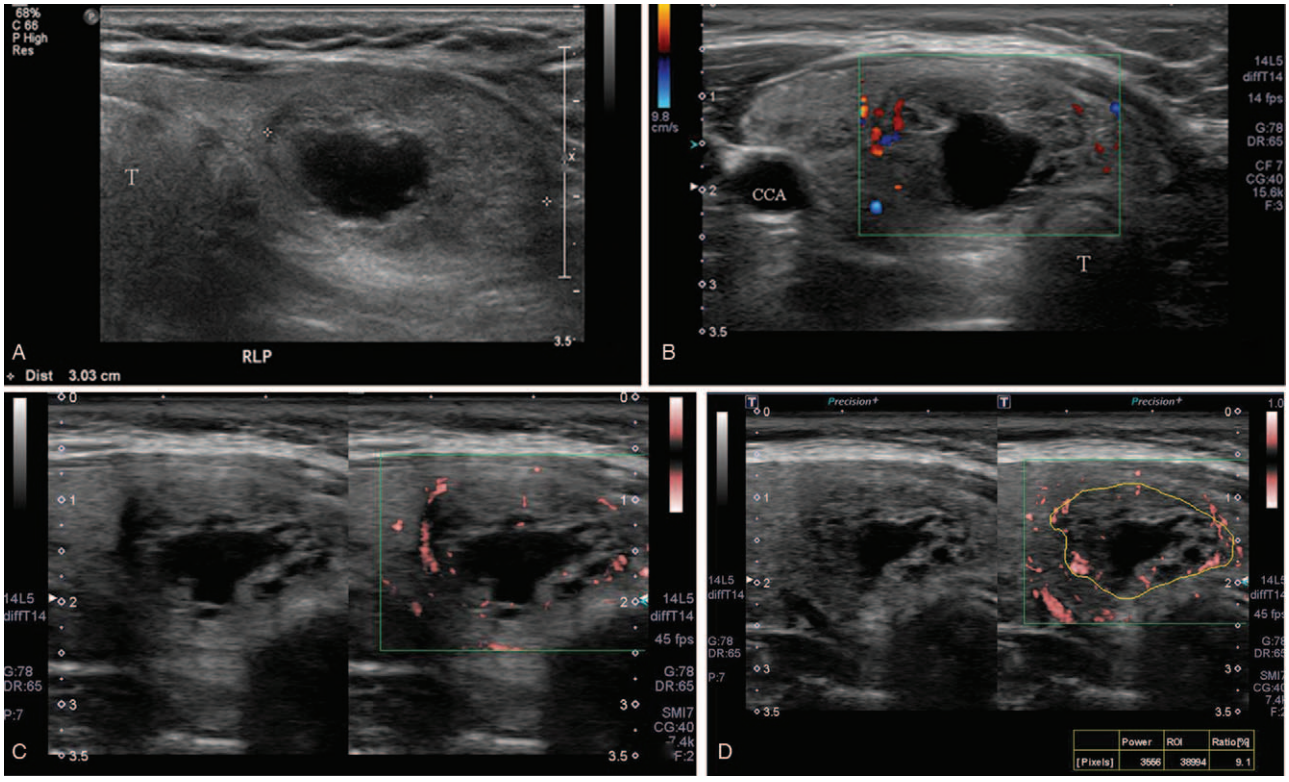

Figure 4. A representative case of a benign nodule. (A) A 52-year-old woman had a 3-cm, low suspicious nodule in the right thyroid lobe. (B), (C) This nodule was visually scored as 2 on color doppler and 2 on superb microvascular imaging. The nodule was scored as 15 on B-mode, B-mode + color Doppler and B-mode + superb microvascular imaging at likelihood of malignancy. (D) Nodular vascularity was 9.1 on pixel count. On fine needle aspiration and biopsy, the nodule was confirmed as a benign follicular nodule. CCA = common carotid artery, T = trachea.

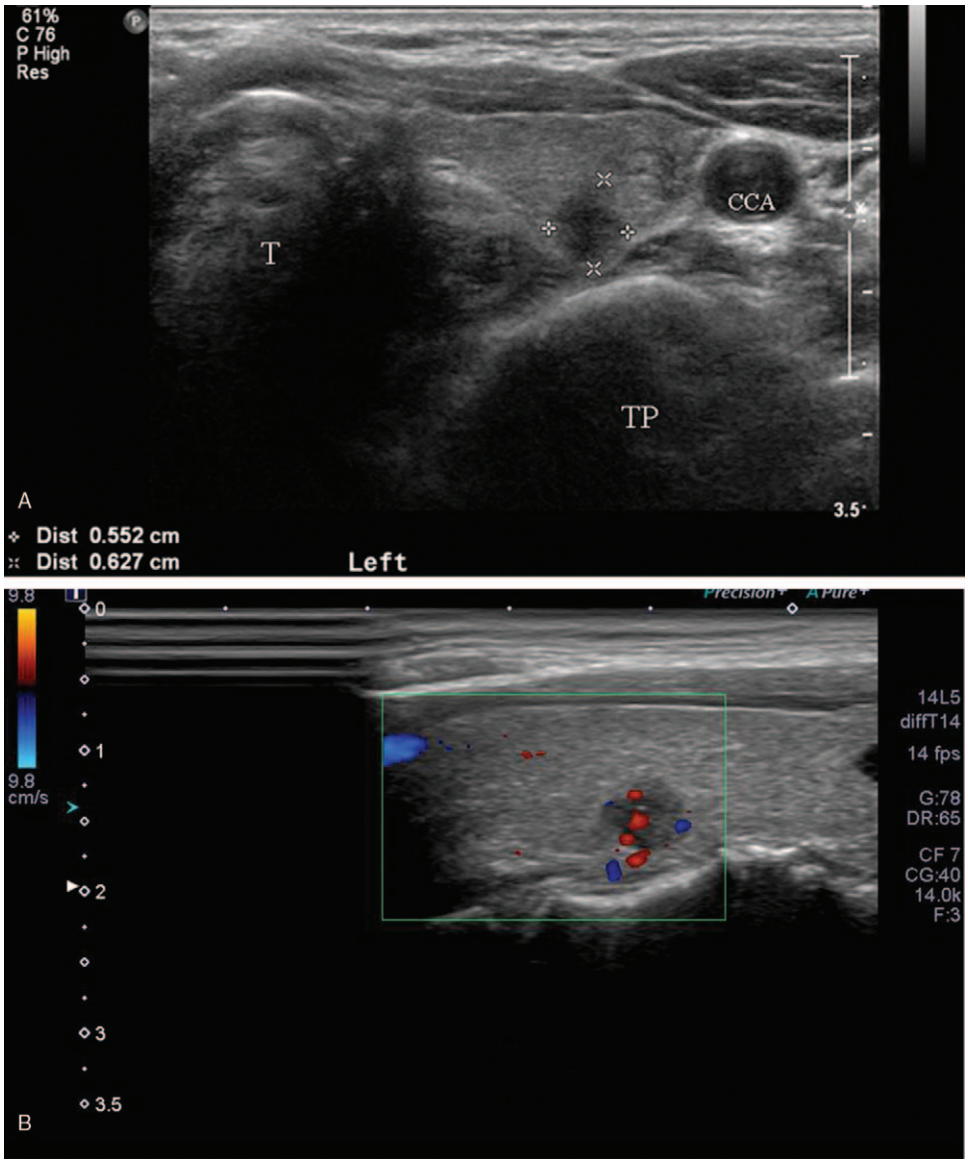

Figure 5. A representative case of a malignant nodule. (A) A 60-year-old woman presented a 0.6-cm, highly suspicious nodule in the left thyroid lobe. (B), (C) This nodule was visually scored as 2 on color doppler and 3 on superb microvascular imaging. The nodule was scored as 80 on B-mode and B-mode + color doppler, however 95 on B-mode + superb microvascular imaging at likelihood of malignancy. (D) Nodular vascularity was 54.8 on pixel count. On fine needle aspiration, the nodule was confirmed as papillary thyroid cancer. CCA = common carotid artery, TP = transverse process of cervical vertebra, T = trachea.

modified Doppler US that extracts flow signals from large-to-small vessels and displays information allowing detailed visualization of slow vascular flow without using a contrast agent.[23] The benefits of this technique include good visualization of a low-velocity flow, high-resolution imaging, minimal motion artifacts, and high frame rate. This allows visualization and quantification of the highly vascular thyroid nodules through the microvasculature from anarchical angiogenesis. Since the introduction of the SMI technique to the medical field, there have been numerous studies on the clinical use of SMI in various diseases of multiple organs. Recently, SMI evaluation using quantitative measurements of Doppler signals has been introduced. SMI quantification using the pixel count employs the percentage ratio between the pixels for the Doppler signal and those for the total lesion.[24,25] Several studies have investigated the diagnostic value of SMI quantification using pixel count in the abdomen and breasts.[26–29] Ra et al[26] evaluated the value and diagnostic performance of adding SMI to conventional US for diagnosing acute cholecystitis and found that the SMI pixel count was significantly higher in acute cholecystitis than in non-acute cholecystitis (169.84 vs 27.48, $P < .001$). Moreover, US + SMI could objectively improve the diagnostic performance compared with conventional US for acute cholecystitis. For breast lesion diagnosis, few studies have reported the diagnostic value of SMI quantification in differentiating between benign and malignant breast masses.[27–29] Zhang et al[27] reported that the mean vascular index was significantly higher in malignant breast mass (9.7 ± 8.2) than that in benign ones (3.4 ± 3.3) ($P < .0001$). Park

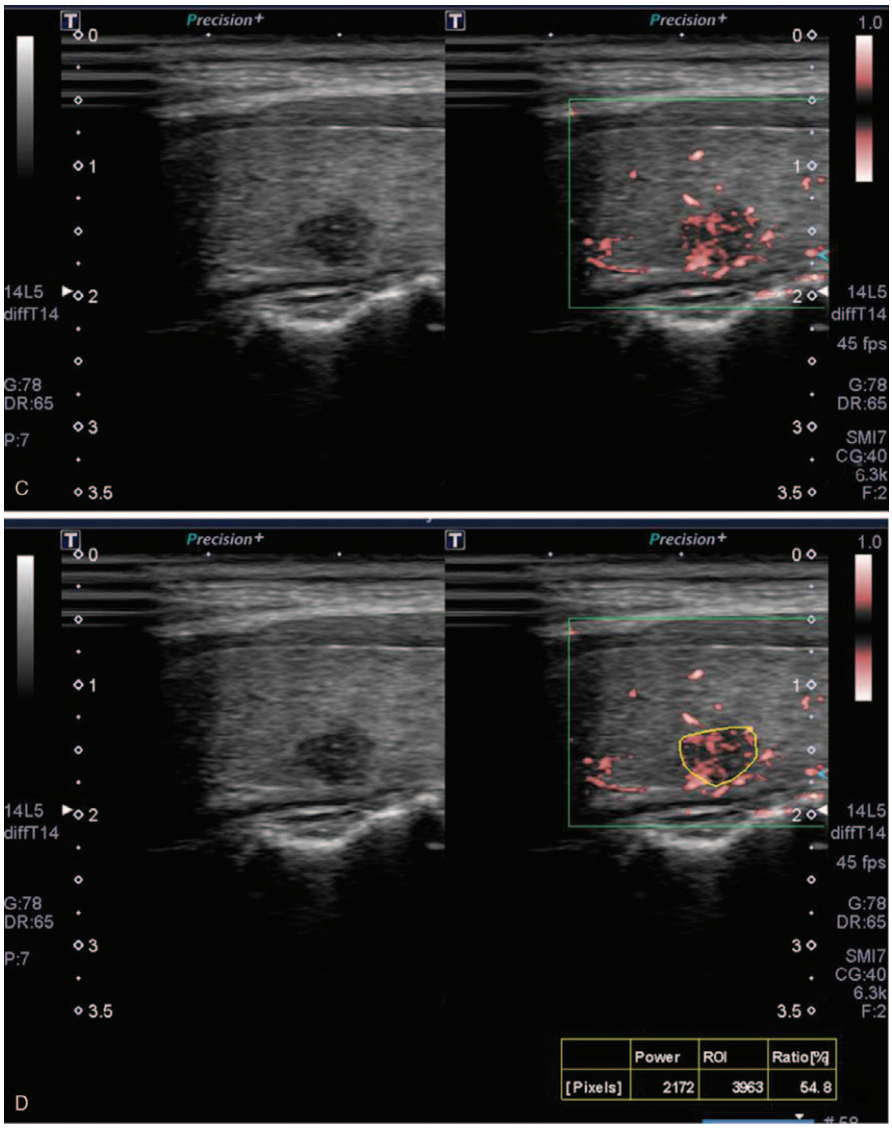

Figure 5. (Continued).

et al[28] suggested an association of malignant breast masses with a higher vascular index (15.1 ± 7.3 vs 5.9 ± 5.6, $P < .0001$) and that adding SMI to B-mode US could prevent unnecessary biopsy of benign masses without sensitivity loss. A more recent study by Lee et al[29] evaluated the diagnostic value of combining the quantitative parameters of shear wave elastography and SMI with breast US to differentiate between benign and malignant breast masses. They found that combined B-mode and SMI vascular index had a significantly higher AUC value (0.778) than B-mode alone (0.719) ($P = .047$). Moreover, B-mode US combined with maximum elasticity, elasticity ratio, and SMI vascular index had the best diagnostic performance of AUC value (0.849). However, to our knowledge, this is the first study to analyze SMI quantification using multiple consecutive cases of thyroid nodules in real clinical practice. In our study, although there was an overlap in the standard deviation of pixel counts between benign and malignant nodules, malignant nodules showed significantly higher values in SMI quantification compared with benign ones. SMI quantification of thyroid nodules could contribute to differentiating between benign and malignant thyroid nodules.

Numerous guidelines have recommended the TIRADS according to the US pattern of thyroid nodules for appropriate malignancy risk stratification.[5–9] In 2016, The Korean Society

Table 3

Vascularity quantification using in-house pixel count software.

Variable	SMI pixel count
Benign (mean ± SD)	10.84 ± 9.47
Malignant (mean ± SD)	17.94 ± 12.53
P value	.038
Sensitivity (%)	40.54*
Specificity (%)	91.3*
AUC	0.643 (0.509–0.763)

AUC = area under the receiver operating characteristic curve, SD = standard deviation, SMI = superb microvascular imaging.

* Cut-off value (maximal value by Youden index) = 17.

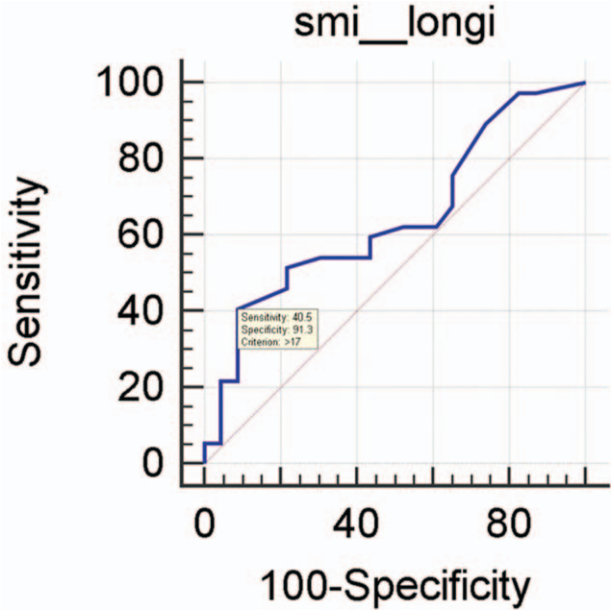

Figure 6. Results of the area under the receiver operating characteristic curve (AUC) of the pixel count of thyroid nodules for differentiating between benign and malignant nodules.

Table 4

Comparison of the SMI pixel count according to the US pattern.

Variable	K-TIRADS 3/4 (n = 45)	K-TIRADS 5 (n = 15)
Benign (mean ± SD)	10.84 ± 9.47 (n = 22)	9.2 (n = 1)
Malignant (mean ± SD)	17.94 ± 12.53 (n = 23)	14.3 ± 13.58 (n = 14)
P value	.038	.723

K-TIRADS = Korean thyroid imaging reporting and data system, SD = standard deviation, SMI = superb microvascular imaging, US = ultrasonography.

of Thyroid Radiology published revised recommendations for US-based diagnosis and management of thyroid nodules.[5] This categorization has been used in clinical practice with the nodules included in this study being analyzed using this categorization. Based on the K-TIRADS, thyroid nodules were categorized as benign (KT2), low suspicious (KT3), intermediate suspicious (KT4), and high suspicious (KT5). In the current study, there was a significant difference in the SMI pixel count between benign and malignant nodules in KT3/4, but not in KT5. Hong et al[30] reported the histologic malignant tumor type according to the K-TIRADS and found that papillary thyroid carcinoma (PTC) was the most common malignancy type in KT5 nodules. Contrastingly, the most common malignancy of KT3 and KT4 nodules was follicular thyroid carcinoma (FTC). PTC and FTC are known to have different US features; therefore, the US tumor patterns provide information regarding the histologic malignancy type.[31,32] PTC is characterized by large proportions of dense fibrosis (up to 89%),[33,34] which may result in the insignificant result of pixel count in KT5 nodules for differentiation of benign and malignant nodules in our study. However, the sample size of KT5 nodules included in this study was too small to yield strong findings and future studies with larger samples should be conducted to validate our findings.

This study has some limitations. First, given the small sample size and retrospective study design, there could have been a selection bias. Moreover, there was a relatively high malignancy proportion of included nodules. This study was conducted at a tertiary university hospital; therefore, most patients had been referred from local clinics or screening centers where they had presented with suspicious findings. Second, 2 reviewers performed the SMI measurements through consensus; therefore, we could not evaluate the reproducibility of SMI quantification. Thus, there is a need for further studies with large populations and inter-observer correlation for SMI quantification. Nevertheless, we believe that this study contributes to the literature, as it is the first study on the quantitative analysis of SMI in thyroid nodules. Third, the ROI size could be affected by the SMI pixel count. We attempted to adhere to the ROI measurement rules and thought that there would be relatively small variations in the SMI pixel count since the ROI was measured within the maximum as large since it did not violate the ROI measurement rules. Additionally, we used the average SMI value of the 3 ROIs to minimize the measurement error.

In conclusion, the inclusion of visual analysis of SMI had a similar diagnostic performance as conventional US in distinguishing between benign and malignant thyroid nodules. Nevertheless, SMI quantification may help differentiate between malignant and benign thyroid nodules, especially in cases of nodules with low-to-intermediate suspicious US features.

Author contributions

Conceptualization: Hye Shin Ahn, Su Min Ha.
Data curation: Hye Shin Ahn, Su Min Ha.
Formal analysis: Hye Shin Ahn, Su Min Ha.
Funding acquisition: Hye Shin Ahn.
Investigation: Min Ji Hong, Hye Shin Ahn.
Methodology: Hye Shin Ahn, Jiyun Oh.
Project administration: Hye Shin Ahn, Jiyun Oh.
Resources: Hye Shin Ahn, Jiyun Oh.
Software: Hye Shin Ahn, Jiyun Oh.
Supervision: Min Ji Hong, Hye Shin Ahn, Hyun Jeong Park.
Validation: Min Ji Hong, Hye Shin Ahn, Hyun Jeong Park.
Visualization: Hye Shin Ahn, Hyun Jeong Park.
Writing – original draft: Hye Shin Ahn.
Writing – review & editing: Min Ji Hong.

References

[1] Han DS, Wu WT, Hsu PC, et al. Sarcopenia is associated with increased risks of rotator cuff tendon diseases among community-dwelling elders: a cross-sectional quantitative ultrasound study. Front Med (Lausanne) 2021;8:630009.
[2] Hsu PC, Chang KV, Wu WT, et al. Effects of ultrasound-guided peritendinous and intrabursal corticosteroid injections on shoulder tendon elasticity: a post hoc analysis of a randomized controlled trial. Arch Phys Med Rehabil 2021;102:905–13.
[3] Moon WJ, Jung SL, Lee JH, et al. Benign and malignant thyroid nodules: US differentiation–multicenter retrospective study. Radiology 2008;247:762–70.
[4] Frates MC, Benson CB, Charboneau JW, et al. Management of thyroid nodules detected at US: society of radiologists in ultrasound consensus conference statement. Radiology 2005;237:794–800.
[5] Shin JH, Baek JH, Chung J, et al. Ultrasonography diagnosis and imaging-based management of thyroid nodules: revised Korean society of thyroid radiology consensus statement and recommendations. Korean J Radiol 2016;17:370–95.
[6] Haugen BR, Alexander EK, Bible KC, et al. 2015 American Thyroid Association Management Guidelines for adult patients with thyroid

nodules and differentiated thyroid cancer: the American thyroid association guidelines task force on thyroid nodules and differentiated thyroid cancer. Thyroid 2016;26:1–133.
[7] Gharib H, Papini E, Garber JR, et al. American Association of Clinical Endocrinologists, American College of Endocrinology, and Associazione Medici Endocrinologi Medical Guidelines for Clinical Practice for the Diagnosis and Management of Thyroid Nodules–2016 Update. Endocrine Practice 2016;22:622–39.
[8] Russ G, Bonnema SJ, Erdogan MF, Durante C, Ngu R, Leenhardt L. European Thyroid Association Guidelines for ultrasound malignancy risk stratification of thyroid nodules in adults: the EU-TIRADS. Eur Thyroid J 2017;6:225–37.
[9] Tessler FN, Middleton WD, Grant EG, et al. ACR thyroid imaging, reporting and data system (TI-RADS): white paper of the ACR TI-RADS committee. J Am Coll Radiol 2017;14:587–95.
[10] Lagalla R, Caruso G, Novara V, Cardinale AE. Flowmetric analysis of thyroid diseases: hypothesis on integration with qualitative color-Doppler study. Radiol Med 1993;85:606–10.
[11] Taylor KJ, Ramos I, Carter D, Morse SS, Snower D, Fortune K. Correlation of Doppler US tumor signals with neovascular morphologic features. Radiology 1988;166:57–62.
[12] Chung J, Lee YJ, Choi YJ, et al. Clinical applications of Doppler ultrasonography for thyroid disease: consensus statement by the Korean Society of Thyroid Radiology. Ultrasonography 2020;39:315–30.
[13] Machado P, Segal S, Lyshchik A, Forsberg F. A novel microvascular flow technique: initial results in thyroids. Ultrasound Q 2016;32:67–74.
[14] Cappelli C, Pirola I, Gandossi E, et al. Ultrasound microvascular blood flow evaluation: a new tool for the management of thyroid nodule? Int J Endocrinol 2019;2019:7874890.
[15] Zhu YC, Zhang Y, Deng SH, Jiang Q. A prospective study to compare superb microvascular imaging with grayscale ultrasound and color Doppler flow imaging of vascular distribution and morphology in thyroid nodules. Med Sci Monit 2018;24:9223–31.
[16] Kong J, Li JC, Wang HY, et al. Role of superb micro-vascular imaging in the preoperative evaluation of thyroid nodules: comparison with power Doppler flow imaging. J Ultrasound Med 2017;36:1329–37.
[17] Cibas ES, Ali SZ. The bethesda system for reporting thyroid cytopathology. Thyroid 2009;19:1159–65.
[18] Jung CK, Min HS, Park HJ, et al. Pathology reporting of thyroid core needle biopsy: a proposal of the Korean endocrine pathology thyroid core needle biopsy study group. J Pathol Transl Med 2015;49:288–99.
[19] Ahn HS, Lee JB, Seo M, Park SH, Choi BI. Distinguishing benign from malignant thyroid nodules using thyroid ultrasonography: utility of adding superb microvascular imaging and elastography. Radiol Med 2018;123:260–70.
[20] Darvish L, Khezri M, Teshnizi SH, Roozbeh N, Dehkordi JG, Amraee A. Color Doppler ultrasonography diagnostic value in detection of malignant nodules in cysts with pathologically proven thyroid malignancy: a systematic review and meta-analysis. Eur J Hum Genet 2019;21:1712–29.
[21] Papini E, Guglielmi R, Bianchini A, et al. Risk of malignancy in nonpalpable thyroid nodules: predictive value of ultrasound and color-Doppler features. J Clin Endocrinol Metab 2002;87:1941–6.
[22] Frates MC, Benson CB, Doubilet PM, Cibas ES, Marqusee E. Can color Doppler sonography aid in the prediction of malignancy of thyroid nodules? J Ultrasound Med 2003;22:127–31. quiz 132-124.
[23] Gabriel M, Tomczak J, Snoch-Ziolkiewicz M, Dzieciuchowicz L, Strauss E, Oszkinis G. Comparison of superb micro-vascular ultrasound imaging (SMI) and contrast-enhanced ultrasound (CEUS) for detection of endoleaks after endovascular aneurysm repair (EVAR). Am J Case Rep 2016;17:43–6.
[24] Park AY, Seo BK. Up-to-date Doppler techniques for breast tumor vascularity: superb microvascular imaging and contrast-enhanced ultrasound. Ultrasonography 2018;37:98–106.
[25] Park AY, Seo BK, Woo OH, et al. The utility of ultrasound superb microvascular imaging for evaluation of breast tumour vascularity: comparison with colour and power Doppler imaging regarding diagnostic performance. Clin radiol 2018;73:304–11.
[26] Ra JC, Lee ES, Park HJ, et al. Efficacy of superb microvascular imaging for diagnosing acute cholecystitis: comparison with conventional ultrasonography. Ultrasound Med Biol 2018;44:1968–77.
[27] Zhang XY, Zhang L, Li N, et al. Vascular index measured by smart 3-D superb microvascular imaging can help to differentiate malignant and benign breast lesion. Cancer Manag Res 2019;11:5481–7.
[28] Park AY, Kwon M, Woo OH, et al. A prospective study on the value of ultrasound microflow assessment to distinguish malignant from benign solid breast masses: association between ultrasound parameters and histologic microvessel densities. Korean J Radiol 2019;20:759–72.
[29] Lee EJ, Chang YW. Combination of quantitative parameters of shear wave elastography and superb microvascular imaging to evaluate breast masses. Korean J Radiol 2020;21:1045–54.
[30] Hong MJ, Na DG, Baek JH, Sung JY, Kim JH. Impact of nodule size on malignancy risk differs according to the ultrasonography pattern of thyroid nodules. Korean J Radiol 2018;19:534–41.
[31] Jeh SK, Jung SL, Kim BS, Lee YS. Evaluating the degree of conformity of papillary carcinoma and follicular carcinoma to the reported ultrasonographic findings of malignant thyroid tumor. Korean J Radiol 2007;8:192–7.
[32] Park JW, Kim DW, Kim D, Baek JW, Lee YJ, Baek HJ. Korean thyroid imaging reporting and data system features of follicular thyroid adenoma and carcinoma: a single-center study. Ultrasonography 2017;36:349–54.
[33] Isarangkul W. Dense fibrosis. Another diagnostic criterion for papillary thyroid carcinoma. Arch Pathol Lab Med 1993;117:645–6.
[34] Carcangiu ML, Zampi G, Rosai J. Papillary thyroid carcinoma: a study of its many morphologic expressions and clinical correlates. Pathol Annu 1985;20 Pt 1:1–44.